INTERNATIONAL JOURNAL OF SPORT BIOMECHANICS, 1989, 5, 258-274

A Multisegment Dynamic Model of Ski Jumping

Mont Hubbard, Robin L. Hibbard, Maurice R. Yeadon, and Andrzej Komor

This paper presents a planar, four-segment, dynamic model for the flight mechanics of a ski jumper. The model consists of skis, legs, torso and head, and arms. Inputs include net joint torques that are used to vary the relative body configurations of the jumper during flight. The model also relies on aerodynamic data from previous wind tunnel tests that incorporate the effects of varying body configuration and orientation on lift, drag, and pitching moment. A symbolic manipulation program, "Macsyma," is used to derive the equations of motion automatically. Experimental body segment orientation data during the flight phase are presented for three ski jumpers which show how jumpers of varying ability differ in flight and demonstrate the need for a more complex analytical model than that previously presented in the literature. Simulations are presented that qualitatively match the measured trajectory for a good jumper. The model can be used as a basis for the study of optimal jumper behavior in flight which maximizes jump distance.

Many analytical models have been made of the flight phase of ski jumping, the earliest by Straumann (1926), whose analytical career spanned nearly four decades (Straumann, 1964). A highly mathematical analysis was performed by Thomas (1971). Work by Krylov and Remizov (1974), and later by Remizov (1984), used a simplified model consisting of a single particle to describe the motion of the jumper/ski system center of mass (CM) and approached the problem from an optimal control point of view. Although their model took into account the first-order effect of the angle of attack (their control variable) on the lift and drag, neither the jumper's rotation nor the effect of body configuration on aerodynamics was included. Ward-Smith and Clements (1982) used an approximately 1/6 scale model jumper in wind tunnel tests. Their later analysis (1983) also relied on a particle model, but, curiously, assumed a *constant* jumper incidence angle

Mont Hubbard and Robin L. Hibbard are with the Department of Mechanical Engineering at the University of California, Davis, CA 95616. Maurice R. Yeadon is with the Biomechanics Laboratory at the University of Calgary, 2500 University Drive N.W., Calgary, Alberta, Canada T2N 1N4. Andrzej Komor is with the Institute of Sport, Warsaw 01-809 Poland.

measured from the relative wind. Thus, although they realized the necessity for maintaining pitching moment near zero through the flight, their model did not account for the effects of pitching moment on the jumper attitude and thus, indirectly, on the flight. Nor did it allow for a changing angle of attack in spite of the fact that Krylov and Remizov (1974) had suggested that the optimal angle of attack was not constant.

Heuristically, ski jumping is an event in which knowledge of three separate types of information should allow the prediction of the jump distance: (a) the takeoff conditions (velocity and positions of the jumper and skis), (b) the aerodynamic characteristics of the jumper/ski system as a function of jumper and ski orientations and the relative wind direction and magnitude, and (c) the muscular controls the jumper exercises during the flight to change his configuration.

Some progress has been made in acquiring information in the first area above. Komi, Nelson, and Pulli (1974) documented takeoff conditions. Dillman, Campbell, and Gormley (1980) used force platforms to measure the jumping ability of ski jumpers in a simulated jumping movement.

Two groups of researchers (Maryniak, 1975; Maryniak & Krasnowski, 1974; Maryniak & Lesniewska, 1978; Tani & Iuchi, 1971) have addressed the effects of jumper configuration on aerodynamics. The paper by Tani and Iuchi (1971) documents extensive wind tunnel studies of a full scale jumper/ski system. Comprehensive measurements were made of lift, drag, and pitching moment as a function of jumper and ski orientation, and the relative wind direction. The jumper/ski system tested was composed of four rigid bodies connected at the ankles, hips, and shoulders. Thus their experimental data set covers nearly the entire spectrum of jumper and ski positions (specified by four angles) likely to be found in a jump and is exactly the information that will be required in a computer simulation of the event using a multilink model.

Maryniak and colleagues (Maryniak, 1975; Maryniak & Krasnowski, 1974; Maryniak & Lesniewska, 1978) all rely on experimental aerodynamic data using a model jumper in a wind tunnel, but limited to only four body configurations. Standard aircraft flight stability techniques are applied to investigate jumper dynamic stability by Maryniak and Krasnowski (1974). The pitching moment about the ski/boot junction is broken into two parts, one due to angle of attack and another to jumper attitude relative to vertical. In Maryniak and Lesniewska (1978) the Boltzmann-Hamel equations are written using a single rigid-body model that accounts for effects of jumper configuration on aerodynamic forces and moments but does not consider jumper configuration from a dynamic point of view.

Rather, configuration angles are chosen as control variables. This approach has the disadvantage that orientations and their rates of change may arise that are in fact impossible for the jumper to achieve in reality. The approach to be presented in this paper, which includes a complete dynamic model for the orientation of each jumper segment, circumvents this difficulty. Conservation of angular momentum, and its effects on achievable jumper orientations, is an explicit feature of our model that has not been addressed in previous models.

Maryniak and Lesniewska (1978) present simulations for the rigid-body model. They suggest that the jumper configuration that maximizes distance is one which, while maintaining pitching moment near zero, also maximizes the lift-to-drag ratio. However, this conflicts with the findings of Krylov and Remizov (1974) that the optimal angle of attack gradually varies over the flight between that for maximum L/D and that which produces maximum lift.

In spite of the fact that thus far no analytical models have included dynamic variations of body configuration, it is widely recognized that the length of flight "is substantially influenced by the skier's posture in the air and by the change of this orientation . . . during the flight" (Remizov, 1984, p. 167) and that "the aerodynamic situation during the flight is also substantially influenced by relative positions . . . of the different body segments and the skis (Watanabe, 1983)," as quoted from Denoth, Luethi, and Gasser (1987, p. 414). The changing orientation of the jumper and ski system as a result of muscle actions results in perturbations in the overall lift and drag forces that change the accelerations experienced by the jumper and affect the center of mass trajectory and resulting jump distance.

In this paper we present a more complex model for the flight phase of ski jumping that extends previous models in this respect. In the next section the jumper is modeled as a collection of planar, rigid bodies. The equations of motion based on a Lagrangian formulation are derived automatically using a symbolic manipulation program ("Macsyma," 1986). The experimental data of Tani and Iuchi (1971) are interpolated to calculate lift, drag, and pitching moment for any body configuration within their ranges. Internal joint torques are calculated that maintain the jumper in a rigid body configuration. Perturbations on these rigid-body maintenance torques change the jumper configuration and control the trajectory. Simulations of the model are presented and compared with experimental data for three jumpers.

Equations of Motion

Figure 1 shows a schematic of the four-link planar model. All motion is assumed to take place in the jumper sagittal plane, which is also assumed to coincide with

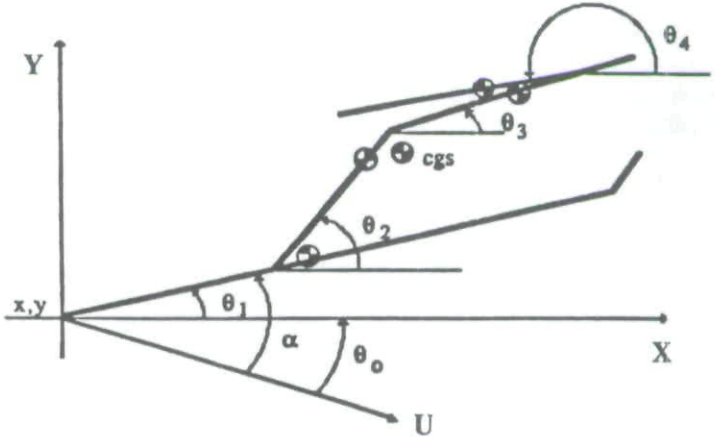

Figure 1 — Schematic of four-link model of ski jumper near beginning of flight. X,Y coordinate system with origin at end of takeoff ramp locates rear tip of skis at position x, y. Four remaining coordinates θ_i i=1,...4, are orientations of links relative to x axis. Flight path angle θ_o is angle of velocity vector of overall CM relative to horizontal and α is the ski angle of attack, the angle between the total velocity vector U and the skis.

the hill's plane of symmetry. The origin of the Cartesian coordinate system is chosen to be at the end of the inrun ramp, with x horizontal forward and y positive up. The model has 6 degrees of freedom: x and y coordinates of the rear tip of the skis to locate the system in the plane, and the four orientation angles of the links (skis, lower extremities, torso–head, and arms) relative to horizontal; θ_i i=1,...4, respectively. The flight path angle θ_o, the angle of the velocity vector of the center of mass (CM) relative to horizontal, is defined as

$$\theta_o = -\tan^{-1} v_y/v_x \tag{1}$$

where v_x and v_y are the components of the velocity vector of the CM.

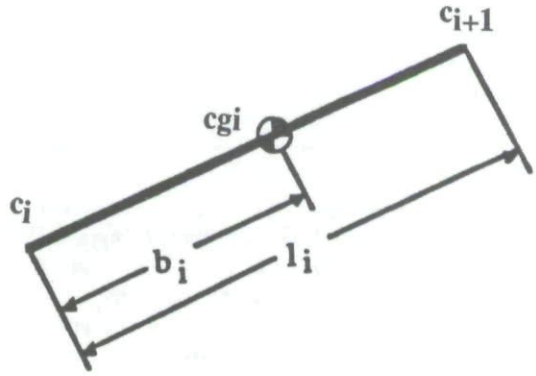

Figure 2 — Schematic of ith link with distances l_i and b_i between joints and from joint to CM, respectively.

Consider the ith link as shown in Figure 2, with length l_i (from connection point c_i with link i−1, to connection point c_{i+1} with link i+1), distance b_i to the CM, mass m_i and centroidal moment of inertia I_i. Then the velocity vector of the CM of the ith link is

$$\mathbf{v}_i = [v_{xi}\ v_{yi}]^T = \mathbf{v}_{ci} + [-\dot{\theta}_i \bullet \sin\theta_i \bullet b_i \quad \dot{\theta}_i \bullet \cos\theta_i \bullet b_i]^T, \tag{2}$$

the velocity of the next connection point c_{i+1} is given by

$$\mathbf{v}_{ci+1} = [v_{xci+1}\ v_{yci+1}]^T = \mathbf{v}_{ci} + [-\dot{\theta}_i \bullet \sin\theta_i \bullet l_i \quad \dot{\theta}_i \bullet \cos\theta_i \bullet l_i]^T, \tag{3}$$

and the position vector of the ith CM is expressed as

$$\mathbf{r}_i = [x_i\ y_i]^T = \mathbf{r}_{ci} + [\cos\theta_i \bullet b_i \quad \sin\theta_i \bullet b_i]^T. \tag{4}$$

The kinetic and potential energies of the ith link are thus

$$T_i = m_i v_i^2/2 + I_i \omega_i^2/2 = m_i v_i^2/2 + I_i \dot{\theta}_i^2/2 \tag{5}$$

and

$$V_i = m_i g y_i = m_i g(y_{ci} + \sin\theta_i \bullet b_i). \tag{6}$$

If we now denote $\mathbf{r}_{co}=[x\ y]^T$ and $\mathbf{v}_{co}=[\dot{x}\ \dot{y}]^T$ and apply recursively Equa-

tions 2 through 6, the Lagrangian $L=T-V$ can be computed as a function of the six coordinates and their derivatives

$$L = \sum_{i=1,\ldots 4} T_i - V_i \tag{7}$$

The differential equations that describe the dynamic changes in the coordinates are then obtained from Lagrange's equations as

$$\frac{d}{dt}\left[\frac{\partial L}{\partial \dot{\mathbf{q}}_i}\right] - \frac{\partial L}{\partial \mathbf{q}_i} = \mathbf{Q}_i \tag{8}$$

where the vector of generalized coordinates is

$$\mathbf{q} = [x\ y\ \theta_1\ \theta_2\ \theta_3\ \theta_4]^T. \tag{9}$$

and $\mathbf{Q}_i$ is the ith nonconservative generalized force, the partial derivative of the virtual work with respect to the ith virtual displacement δq_i (Greenwood, 1965). The nonconservative force terms $\mathbf{Q}_i$ on the right sides of Equation 8 are due to aerodynamic effects (lift, drag, and pitching moment) as well as jumper muscle joint torques. Their calculation will be discussed in further detail below.

Manual implementation of Equations 7 and 8 is extremely tedious and prone to error. However, there are symbolic programs (Macsyma, 1986) that can perform the iterative calculations in Equations 2 through 7 and the differentiations in Equation 8 with respect to both time and the generalized coordinates and their derivatives (e.g., see Leu & Hemati, 1986). Thus the entire left sides of the equations of motion may be derived automatically by specifying to Macsyma only the information in Equations 2 through 6. Furthermore, the Macsyma program is capable of generating Fortran code that can be easily incorporated into a different computer program to solve the equations of motion. The Macsyma program was written to compose the equations for an arbitrarily long n-link chain. This approach is flexible enough to allow adding more links to the model easily. Because the resulting equations for even the four-link model are too lengthy to be included here (the Macsyma program and all output expressions encompassed 13 pages), the reader is referred to Hibbard (1988) for more details.

Aerodynamic Forces and Moments

Tani and Iuchi (1971) measured the aerodynamic forces (lift and drag) and pitching moment experienced by a jumper as a function of body configuration. In wind tunnel tests with a rigid full-scale model, they measured lift, drag, and pitching moment coefficients (relative to the CM of the jumper/ski system) as a function of body position and relative wind angle. It should be noted that the model described here and all the simulations assume a motionless atmosphere, that is, no wind. In this case the relative wind is simply the opposite of the jumper's translational velocity. It would be straightforward to include the effects of wind if this were desired. However, measurement of winds at all points along the trajectory is extremely difficult.

The lift and drag forces are given by

$$\mathbf{L} = [L\sin\theta_o,\ L\cos\theta_o]^T \tag{10a}$$

$$\mathbf{D} = [-D\cos\theta_o,\ D\sin\theta_o]^T \tag{10b}$$

The total aerodynamic force, denoted by **F**, is the sum of the lift and drag

$$\mathbf{F} = \mathbf{L} + \mathbf{D} \tag{11}$$

Figure 3 shows the configuration variables investigated by Tani and Iuchi (1971). Clearly the four variables α, σ, θ, and ϕ are simply related to the state variables in the present dynamic model by the relations

$$\alpha = \theta_0 + \theta_1 \quad \theta = \theta_2 - \theta_1 \quad \sigma = \theta_2 - \theta_3 \quad \phi = \theta_3 - \theta_4. \tag{12}$$

In the computation of aerodynamic forces for our model, the system was considered to be a quasi-rigid body with an average translational velocity equal to that of the CM and with zero total angular velocity. Relative motion of the segments means that the actual velocity of each segment differed somewhat from that of the CM. Nonetheless, during most of the flight phase the link angular velocities and translational velocities of the links relative to the CM are small so that the errors in velocities due to the quasi-rigid approximation are typically less than 0.5%. During the initial phase of flight, the transition from the inrun to the flight position, these errors in velocities of the links can be somewhat larger (on the order of 10%), but some are larger and some are smaller, so the average error in local dynamic pressure was still expected to be less than 2 or 3%.

Modifications of the data of Tani and Iuchi (1971) were needed to adapt it to the present model because the generalized coordinates chosen require the application of external forces to one of the links rather than to the body as a whole. This was accomplished with an equipollent system (see Figure 4) of forces and pitching moments that were applied at the rear tip of the skis.

It can then be shown that the generalized nonconservative force vector **Q** whose elements are the right sides of Equation 8 is given by

$$\begin{aligned}\mathbf{Q} = [&-D\cos\theta_o - L\sin\theta_o,\ -D\sin\theta_o + L\cos\theta_o,\\ &PM + PM^* - T_a,\ T_a - T_h,\ T_h - T_s,\ T_s]^T\end{aligned} \tag{13}$$

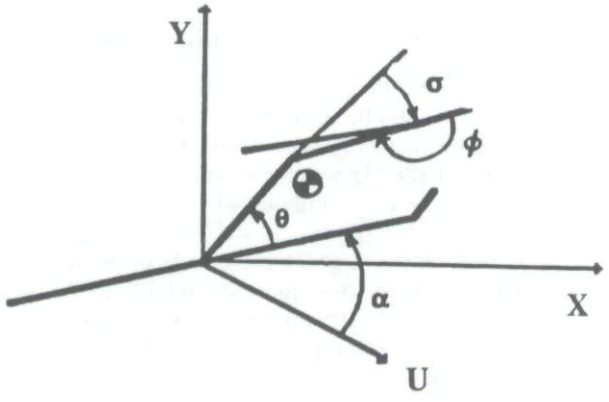

Figure 3 — Effects of jumper configuration variables α, θ, σ, ϕ on aerodynamic forces and moment were investigated by Tani and Iuchi (1971).

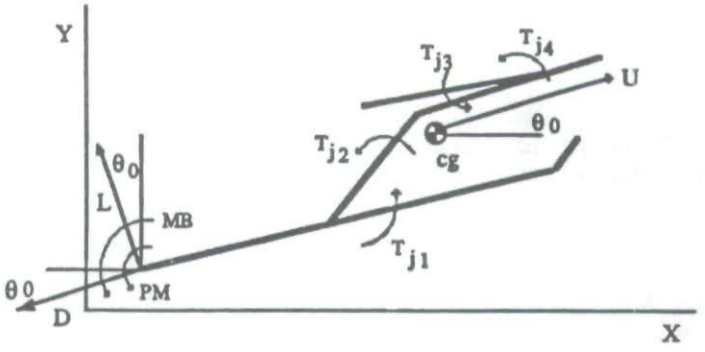

Figure 4 — Model schematic with applied aerodynamic forces and moments. Experimental force system equipollent to that of Tani and Iuchi (1971) was applied to rear tip of skis, requiring an additional moment MB. Also shown are net torques on each link due to jumper joint torques at ankles, hips, and shoulders.

where T_a, T_h, and T_s denote ankle, hip, and shoulder extension torques exerted by the jumper; L, D, and PM are the aerodynamic forces and moment measured by Tani and Iuchi (1971); and PM* accounts for the moment of the aerodynamic force **F**, when it acts at the *system* center of mass, about the rear tip of the skis

$$PM^* = |\mathbf{r}^* \times \mathbf{F}| \tag{14}$$

where

$$\mathbf{r}^* = \mathbf{r}_{cm} \tag{15}$$

Although we do not express it here, clearly $\mathbf{r}_{cm}$ can be calculated from the elements of **q**. The terms in Equation 13 were added to the right side of Equation 8 manually. The complete set of six second-order, coupled differential equations may then be written in functional matrix form as

$$A(\mathbf{q})\ddot{\mathbf{q}} + B(\mathbf{q},\dot{\mathbf{q}})\dot{\mathbf{q}} + C(\mathbf{q})\mathbf{q} = \mathbf{Q} \tag{16}$$

In Equation 16 the dependence of the coefficient matrices A, B, and C on the generalized coordinates and their derivatives is made explicit. Equation 16 was solved by inverting the matrix A numerically at each time step in the simulation. Symbolic inversion using Macsyma was attempted but abandoned. Apparently, symbolic inversion of a very complicated 6x6 matrix is on the ragged edge of achievable tasks for this program.

Although Equation 16 accounts for the effects of the jumper applied joint torques on the evolution of body configuration and ultimately on the trajectory of the jumper CM, it is somewhat difficult to specify torques that result in a given dynamic configuration. A similar but more pronounced difficulty was experienced in a previous model for the pole vault (Hubbard, 1980). Through inverse dynamics techniques, the joint forces and moments required to hold the jumper rigid were computed (Hibbard, 1988). These can then serve as a baseline or datum on which additional perturbation joint torques can be superimposed when relative accelera-

tions of the links are desired. This is not to say that superposition holds, since the differential equations are plainly nonlinear. Rather it is simply convenient to use the rigid torques as a datum so that only the perturbation torques need be specified rather than the entire torques.

This model of jumping based on first principles has an important advantage: body motions that result from the model are guaranteed to be obtainable in actual practice. The variation of aerodynamic forces throughout the time of flight is accomplished by calculating a new set of aerodynamic force and moment coefficients at each integration time step, based on the body segment angles and the flight path angle at each instant. Therefore no matter what body configurations result from a simulation, they are guaranteed to satisfy restrictions on angular momentum from the pitching moment equation and not to violate physical principles. Without constraints on the various body angles, anatomically impossible configurations may still occur, but these additional constraints are easily implemented numerically. Such constraints in fact play a large role in present optimization studies using the model.

Experimental Results

Experimental data were gathered for the 70-m individual ski jumping competition at the 1988 Winter Olympic Games in Calgary. Fifty-eight jumpers were filmed in the two rounds of competition using two Locam 16-mm cameras mounted on tripods with pan and tilt heads. The cameras were operated at approximately 50/fps. Camera location and numerous control point locations in the fields of view were surveyed prior to the competition. The images of wrists, shoulders, hips, ankles, and ski tips were digitized manually in addition to two control points in each frame. The three-dimensional locations of these body landmarks were then determined. The angles of the planar model were obtained by projection of the three-dimensional coordinates on the vertical plane of symmetry bisecting the jumping hill. For further details regarding film analysis techniques, the reader is referred to Yeadon (1989).

Shown in Figure 5 is a comparison of kinematic data for three jumpers of widely varying abilities (the first place and last place finishers, and a jumper whose performance was exactly halfway between them). The jumpers' anthropometric data and overall performance in the competition are summarized in Table 1. The velocities in Table 1 are those measured officially in the competition using photocells just above the takeoff point. The final placings are based on the combined score of two jumps. Jumper P.U. jumped about 85 m in the first round. He should therefore not be regarded as a jumper of average distance but rather as one who had a worse than average (for him) jump in the second round.

One row (two graphs) in Figure 5 is devoted to each jumper, best jumper on top and worst on the bottom. The left column presents the evolution of body configurations versus time. Plotted are the angles of the four segments of the jumper/ski system as previously defined (θ_i, $i=1,\ldots4$), that is, the angles of the skis, legs, torso, and upper extremities relative to horizontal. In the legends of Figures 5, 7, and 8, these four angles (θ_i, $i=1,\ldots4$) are referred to as AS, AL, AT, and AU, respectively. Time $t=0$ is defined to be the moment when the mass center of the jumper/ski system lay in the plane $x=0$, that is, the plane of the vertical concrete slab ending the takeoff ramp. Thus $t=0$ corresponds to the same

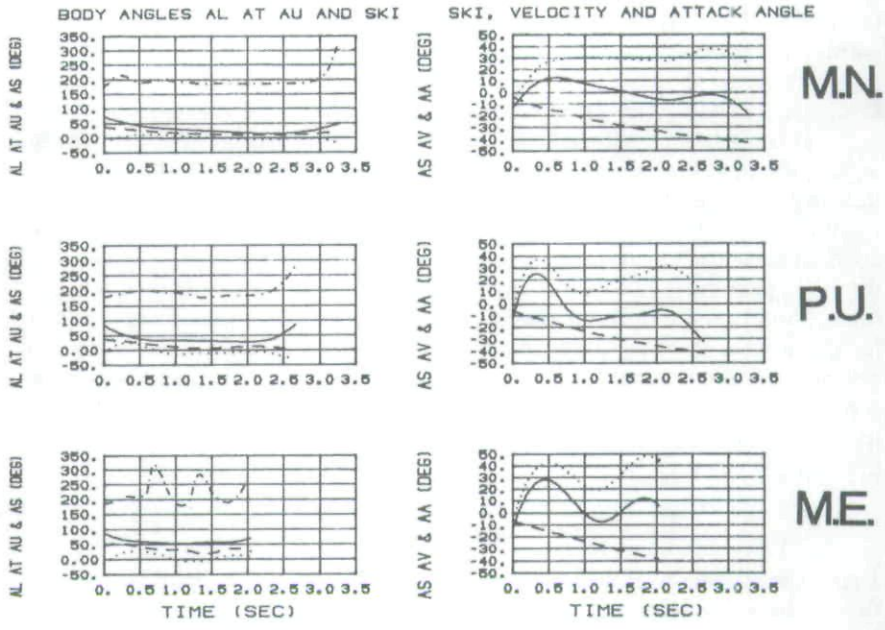

Figure 5 — Experimental ski and body segment orientations versus time for three jumpers at 1988 Calgary Olympic 70-m ski jump. Plotted are the angles of the four segments of the jumper/ski system (θ_i i=1,...4), the angles of the skis, legs, torso, and upper extremities relative to horizontal. In the legend of this figure and Figures 7 and 8, the four angles, θ_i i=1,...4, are referred to as AS, AL, AT, and AU, respectively. Left column: ski ·····, leg _____, torso __ __ __, and arm __.__.__ angles vs. time. Right column: ski angle _____, flight path angle __ __ __, and ski angle of attack ·····. Top, best jumper M.N.; middle, intermediate jumper P.U.; bottom, worst jumper M.E.

Table 1

Jumper Anthropometric and Official Performance Data

Jumper	Height m	Weight kg	Jump distance m	Inrun speed m/s	Finish place of 58
M.N.	1.77	60	89.5	24.2	1
P.U.	1.76	61	72.0	24.2	30
M.E.	1.73	73	55.0	24.1	58

horizontal location for each jumper. All jumpers were airborne by this time. The final time, which varies between jumpers, is the time of touchdown of the feet, not the ski tips, that is, the first time when the skis are in contact with the hill along their entire length.

At t=0 the initial configurations of the three jumpers are not too different from one another. The measured takeoff conditions are summarized in Table 2. Note that our velocities agree to within 0.4 m/s (2%) with the official speeds from Table 1. The ski angle θ_1 for all three jumpers begins near $-11°$, the angle of the inrun slope at takeoff. Initial leg angles θ_2 were 72, 83, and 86° for the best jumper M. Nykanen (M.N.), the intermediate jumper P. Ulaga (P.U.), and the worst jumper M. Edwards (M.E.), respectively. Initial torso angles were 37, 37, and 46° (in the same order), while the angles of the arms were very similar: 174, 178, and 174°. Notice that the best jumper is initially in a significantly lower drag configuration with a lower leg angle and low torso angle. The worst jumper has leg and torso angles 14 and 9° larger, respectively, than those of the best jumper.

Table 2

Measured Takeoff Conditions for Three Jumpers

Jumper	v_x (m/s)	v_y (m/s)	θ_1 (°)	θ_2 (°)	θ_3 (°)	θ_4 (°)
M.N.	23.8	−1.8	−13	72	37	174
P.U.	23.8	−2.6	−12	83	37	178
M.E.	24.0	−2.9	−13	86	46	174

The horizontal components of takeoff velocity differed by less than 1% (these are largely controlled by the officials who set the height of the inrun initiation). Although the aerodynamics of the inrun crouch position have a strong effect on the tangential takeoff velocity as well, apparently even the poorest jumpers have mastered this technique. However, the normal components varied substantially due to differences in the strength of the jump: −1.8, −2.6, −2.9 m/s. Thus the best jumper had a 1.1 m/s larger vertical takeoff velocity than the poorest jumper. Our sensitivity studies, holding all other factors constant, show that this vertical takeoff velocity differential increases jump distance in the neighborhood of 7 m. The additional differences in range must be due to aerodynamic effects in flight. As will be clear from the explanation of the flight data presented in Figure 5, the best jumper M.N. exhibited a much cleaner, more efficient aerodynamic flight configuration.

In spite of the fact that initial takeoff positions varied only within the range of 10–15°, much larger differences are apparent in flight. The most striking feature of the best jumper's configuration history is how nearly parallel his skis, legs, and torso are during the middle 2 seconds of flight, the angles of these seg-

ments differing by only about 20° throughout this period. The legs and skis rotate during the first 0.5 sec to align themselves with the torso, which is pitching forward more slowly. Thus the rapid transition to the flight configuration is achieved by the motion of legs and skis, and to a lesser extent the torso. Note the fine, relatively high frequency control exercised by the arms during the first 1.0 sec of flight as the angular momentum is trimmed and the configuration is adjusted to one with a very small pitching moment. The classically damped overshoot in the arm motion is reminiscent of the optimal response of an automatic control system. Finally note that the excellent flight position is held as long as possible with a very rapid transition to the landing configuration (measured by the time for the arms to go from 200 to 300°) achieved in about 0.3 sec. The flight duration was more than 50% greater than that achieved by the weakest jumper.

The intermediate jumper P.U. exhibited a lower frequency controlling motion of the arms and thus took longer (about 1 sec) to stabilize in a good flight configuration. Nevertheless this was less efficient and stable than that of the best jumper, the angle between the legs and skis during midflight varying in the range of 30 to 40°. The weaker landing transition also took slightly longer to execute (about 0.4 sec). The weakest jumper M.E. never established a stable flight configuration, with large oscillations of the arms (140°), skis (30°), and torso (15°) apparent throughout the flight.

The three graphs at the right of Figure 5 show three variables closely related to the aerodynamics: the angle of the velocity vector θ_0, the angle of the skis θ_1, and the difference between these two—the angle of attack α of the skis, one of the main variables on which the aerodynamic force and moment data of Tani and Iuchi (1971) depend.

For the best jumper the ski angle of attack begins negative, rises abruptly, and remains extremely constant near 30° through much of the flight, increasing to near 40° only near the end of the trajectory. Although more oscillatory, this behavior is qualitatively similar to the optimal angle of attack computed by Krylov and Remizov (1974) and shown in Figure 4 of Remizov (1984), which they predicted should gradually rise throughout the flight. The initial overshoot of the skis of the intermediate jumper, shown more dramatically in the right graph, incurred much deleterious early drag and the ski angle of attack never effectively stabilized. In the case of the poorest jumper, the more nearly vertical body configuration (the minimum leg angle was only 50°) incurred such large drag that the flight ended after only 2.0 sec.

Simulation Results

Not only are the experimental results in Figure 5 indicative that the more complex model presented in this paper is warranted, but they may also be used to partially validate the model. However, a complete validation is possible only through the following procedure:

1. Jumper body segment masses, lengths, and inertias are measured.
2. Jumper joint torques, body configuration, and trajectory are measured as functions of time throughout an entire flight.
3. The inertial data and joint torques are used as input for a simulation, and the resulting simulated configurations and trajectory are compared to the

experimentally measured ones. The closeness of agreement of the simulated and measured data can then be a measure of the model's validity.

Clearly it is impossible to measure joint torques directly. Rather they can only be inferred from a measurement of body configuration time histories and "inverse dynamics" methods. In fact we have used our model in this way to estimate both the aerodynamic forces as well as the joint torques from the experimental flight data of Figure 5. It proves very little, however, to simply play these torques back through the same model. We have therefore avoided this "validation" exercise. It should be clear from this discussion that we believe it is not possible to completely validate any whole-body motion model that includes joint torques as inputs, simply because it is not possible to measure these quantities directly.

Rather, the focus of our simulations has been to learn more about the details of ski jumping than has been possible with more limited models. Before exercising the full complexity of the model, we experimented with several rigid-body flights to study the effects of initial conditions. For example, a search through the data of Tani and Iuchi (1971) yields the configuration that maximizes the lift-to-drag ratio. This configuration may be a first approximation to the dynamic configuration which maximizes distance. Figures 6, 7, and 8b show the simulated results of a flight of a rigid jumper near this configuration (α varies in flight but $\sigma=20°$, $\theta=20°$, and $\phi=165°$).

Jumper parameters (nearly those of M.N.) and initial conditions used in the simulation are shown in Table 3. Although they were not measured, body segment lengths and moments of inertia were estimated using the technique of Dempster and Gaughran (1967) based on the total mass and height measurements for M.N. obtained in Calgary. The remaining initial conditions required for simulation of a rigid jumper are the initial rigid body angular and translational velocities. The initial angular velocity was chosen to maximize the range. The only jumper joint torques applied in the simulation were those required to maintain the body rigid.

Figure 6 depicts the trajectory of the jumper while Figure 7 depicts the time histories of various angles. Also shown in Figure 7 are the rotational effects of the aerodynamic pitching moment on the total angular momentum in flight.

Table 3

Simulated Jumper Anthropometric Data and Takeoff Conditions for Rigid Flight

Height	Body weight	Equipment weight
m	kg	kg
1.77	60	12.5

Takeoff conditions						
v_x (m/s)	v_y (m/s)	θ_1 (°)	θ_2 (°)	θ_3 (°)	θ_4 (°)	ω_o (rad/s)
23.7	0	30	50	30	225	−0.34

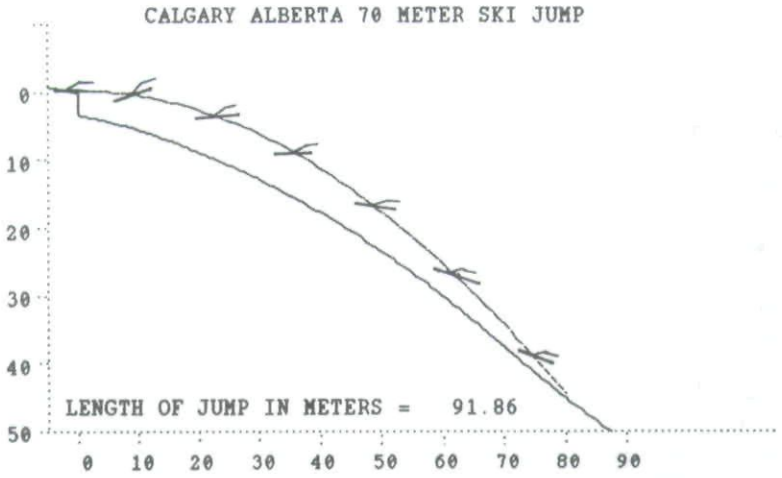

Figure 6 — Jumper trajectory and stick figure schematic during simulated rigid body flight, yielding 91.86-m distance.

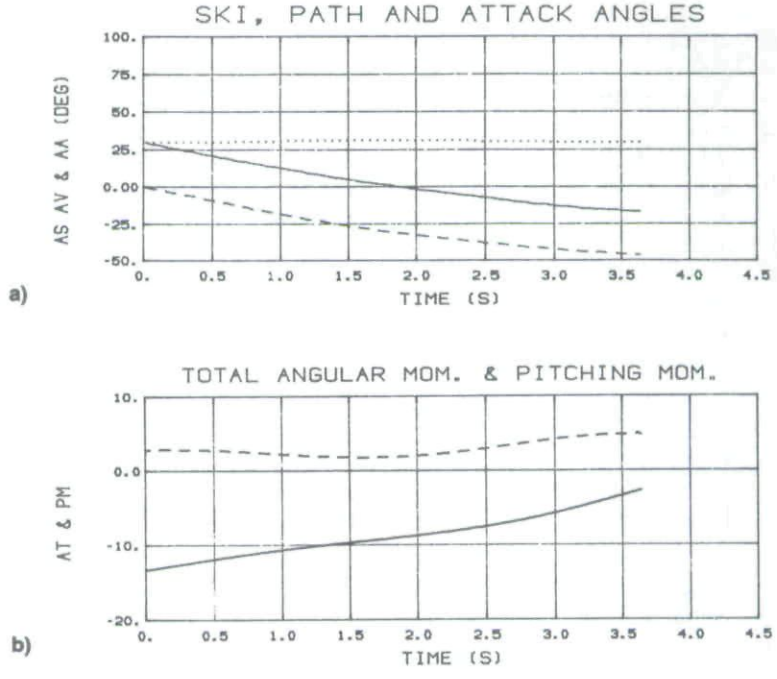

Figure 7 — Simulation results for rigid jumper flight shown in Figure 6: (a) ski angle _____, flight path angle __ __ __, and ski angle of attack ····· vs. time, (b) total angular momentum _____, and pitching moment __ __ __ vs. time.

The simulation obtained a distance of 91.9 m in a time of 3.62 sec, both slightly greater than the distance and time of M.N.'s Olympic jump.

Figure 8 compares ski, leg, and torso angles for three flights for jumper M.N., one actual flight and two simulations. Shown in Figure 8a are the experimental data of the actual jump of M.N. previously presented in Figure 5. Figure 8b shows the ski, leg, and torso angles versus time from the rigid-body simulation of Figures 6 and 7. Figure 8c contains the results of a simulation in which body configuration varies in time. The joint torques for this simulation

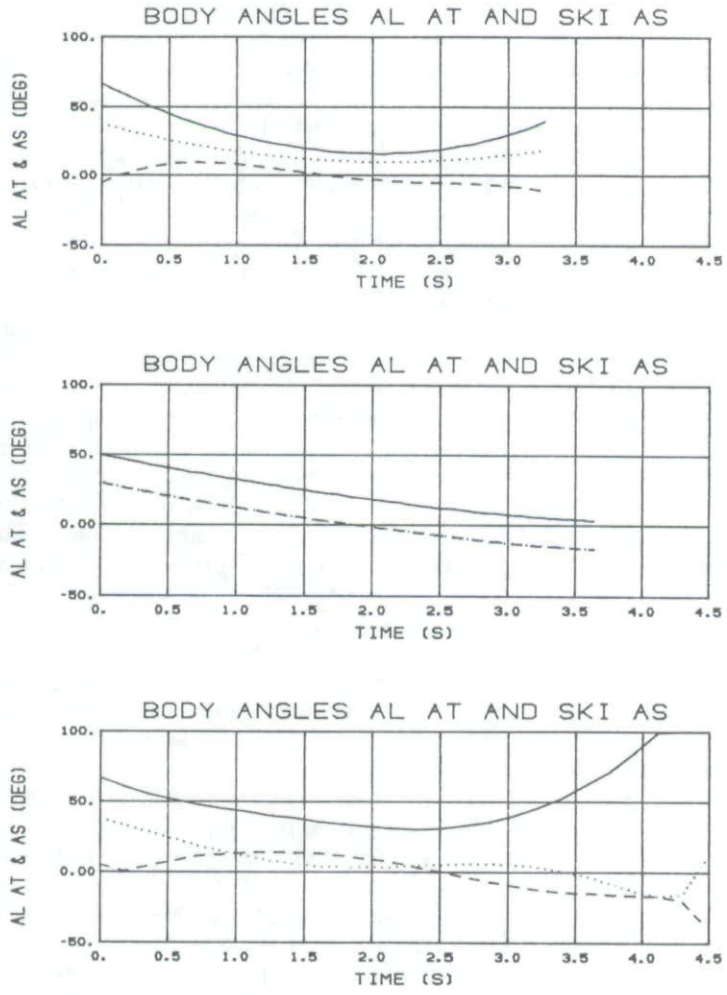

Figure 8 — Comparison of angles of skis ·····, legs _____, and torso _ _ _ for three jumps: (a) actual Olympic flight of jumper M.N.; (b) simulation of rigid body flight for M.N. of Figures 6 and 7, and (c) simulation of preliminary optimized flight for M.N. (body configuration varies during flight).

were generated by an optimization procedure that attempts to maximize jump distance. The optimized flight-path time histories of Figure 8c show many similarities to those of the actual flight, but the time of flight (4.4 sec) and jump distance (95.3 m) are 38% and 6% larger, respectively, than those of the actual flight of the Olympic champion.

Discussion and Conclusions

In attempting to obtain simulated trajectories that were similar to those measured experimentally, we found several inadequacies in the experimental aerodynamic data of Tani and Iuchi (1971). First, given a constant set of initial conditions, the largest determinant of jump distance should be the overall ratio of aerodynamic to gravity forces. This overall ratio appears to have changed gradually over the 17 years since the experimental wind tunnel tests of Tani and Iuchi were completed, perhaps due to several rule changes that have since gone into effect. Skis today are both wider and longer, and innovations have occurred in jumper suit design. All these changes have increased the effects of aerodynamics and increased jump distance.

Second, although the aerodynamic data of Tani and Iuchi (1971) agree with the data of Maryniak and Krasnowski (1974) (the two studies contained one common jumper configuration, which is convenient for comparison), lift and drag forces from the latter study are consistently factors of 1.3 larger and 0.85 smaller, respectively, than those from the former. Additionally, as previously mentioned, we used inverse dynamics techniques and the equations of our model to estimate the lift force for jumper M.N. These data were also about 1.2 times larger than those of Tani and Iuchi at the same body configurations. We believe this accounts for the fact that, using the measured initial conditions and jumper body parameters and the original aerodynamic data of Tani and Iuchi, we were unable to obtain simulated jump distances as great as the measured jump distances. Thus all the simulations shown in this paper have the lift of Tani and Iuchi adjusted by a factor of 1.2, and the drag by a factor of 0.85.

Finally, we have observed time-varying trimming pitching moments, especially in the experimental flight data of jumper M.N. Although these are suggested from the arm oscillations shown in Figure 5 and were discussed previously, they are much more apparent from the estimation of pitching moments that were generated from the derivative of total angular momentum obtained from the experimental data. The wind tunnel experimental data of Tani and Iuchi (1971) and of Maryniak and Krasnowski (1974) do not take into account these trimming pitching moments that were observed in the measured trajectory data.

In order to make our future simulations more meaningful, we believe that more current aerodynamic data must be utilized. This can either be obtained from comprehensive wind tunnel tests recently completed by Maryniak et al. (1989) or may require additional wind tunnel tests to be conducted.

Using the model we have presented, it is possible to compute the set of muscle joint torques as functions of time that will change the body segment orientations in a prescribed manner. This will eventually provide a better understanding of how the aerodynamics of the jumper/ski system are affected by changing body positions in flight and how the jumper can exert muscle joint torques in

order to position himself to obtain the "optimal" flight trajectory, which will lead to the longest jump distance. The model should be able to replicate Remizov's work by constraining the motion to that of a rigid body, and also extend it by understanding what can be gained by allowing relative motion of the body segments. The difficulties in such optimization studies as recently discussed by Denoth, Luethi, and Gasser (1987) are not to be underestimated.

One possible extension of the model would be adding the hands as a fifth link (a logical extension because the hands are used by experienced jumpers as ailerons and flaps for additional control during flight) in an attempt to model the high frequency trimming moments that were discussed previously. Another long-range goal may be to conduct further wind tunnel experiments to obtain a better model of the aerodynamic forces on ski jumpers.

References

Dempster, W.T., & Gaughran, G.R.L. (1967). Properties of body segments based on size and weight. *American Journal of Anatomy*, **120**, 33-54.

Denoth, J., Luethi, S.M., & Gasser, H.H. (1987). Methodological problems in optimization of the flight phase in ski jumping. *International Journal of Sport Biomechanics*, **3**, 404-418.

Dillman, C.J., Campbell, K.R., & Gormley, J.T. (1980). Force platform testing of ski jumpers. *Journal of U.S. Ski Coaches Association*, **3**(4), 35-38.

Greenwood, D.T. (1965). *Principles of dynamics*. Englewood Cliffs, NJ: Prentice-Hall.

Hibbard, R.L. (1988). *A multi-link model of a ski jumper*. Master's thesis, University of California, Davis.

Hubbard, M. (1980). Dynamics of the pole vault. *Journal of Biomechanics*, **13**, 965-976.

Komi, P.V., Nelson, R.C., & Pulli, M. (1974). *Biomechanics of ski jumping. Studies in sport, physical education and health* (Vol. 5). Jyväskylä: University of Jyväskylä.

Krylov, I.A., & Remizov, L.P. (1974). Problem of the optimal ski jump. *Prikladnaia Matematika i Mekhanika*, **38**, 765-767.

Leu, M.C., & Hemati, N. (1986). Automated symbolic derivation of dynamic equations of motion for robotic manipulators. *ASME Journal of Dynamic Systems, Measurement and Control*, **108**(3), 172-179.

Macsyma™ Reference Manual. (1986). Cambridge, MA: Symbolics, Inc.

Maryniak, J. (1975). Static and dynamic investigations of human motion. *Mechanics of biological solids*. Varna: Bulgarian Academy of Sciences.

Maryniak, J., & Krasnowski, B. (1974). Balance and longitudinal stability of a ski-jumper in flight [in Polish]. *Mechanika Teoretyczna i Stosowa*, **3**, 12.

Maryniak, J., & Lesniewska, A. (1978). Mathematical modelling of ski-jumper flight with the use of Boltzmann-Hamel equations [in Russian]. *Biomechanics*. Sofia: Bulgarian Academy of Sciences.

Maryniak, J., et al. (1989). *Wind tunnel investigation of ski jumper flight*. Unpublished master's thesis, Technical University of Warsaw.

Remizov, L.P. (1984). Biomechanics of optimal flight in ski-jumping. *Journal of Biomechanics*, **17**(3), 167-171.

Straumann, R. (1926). Vom Skiweitsprung und seiner Mechanik. *Jahrbuch des sweicherischen Ski Verbandes*, 34-64.

Straumann, R. (1964). Ski jumping style, flight paths and their evaluation. *Sport*, **71**, 9.

Tani, I., & Iuchi, M. (1971). Flight-mechanical investigation of ski jumping. In K. Kinoshita (Ed.), *Scientific study of skiing in Japan* (pp. 35-52). Tokyo: Hitachi, Ltd.

Thomas J. (1971). *Mathematische Theorie der Aerodynamik des Skiflug*. Berlin: Akademie-Verlag.

Ward-Smith, A.J., & Clements, D. (1982). Experimental determination of the aerodynamic characteristics of ski-jumpers. *Aeronautical Journal*, **86**, 384-391.

Ward-Smith, A.J., & Clements, D. (1983). Numerical evaluation of the flight mechanics and trajectory of a ski-jumper. *Acta Applicandae Mathematicae*, **1**, 301-314.

Watanabe, K. (1983). Aerodynamic investigation of arm position during the flight phase in ski jumping. In H. Matsui & K. Kobayashi (Eds.), *Biomechanics VIII-B*, (pp. 856-860). Champaign, IL: Human Kinetics.

Yeadon, M.R. (1989). A method for obtaining three-dimensional film data on ski jumping using pan and tilt cameras. *International Journal of Sport Biomechanics*, **5**, 238-247.

Acknowledgments

Portions of this work were supported by a financial grant from the U.S. Olympic Committee. Additionally, the support of the IOC Medical Commission and the Canadian Natural Sciences and Engineering Research Council, and the cooperation of the International Ski Federation and CTV Television, are gratefully acknowledged. This study was also made possible through the support of the following sponsors: Red Lake Corporation, XV Winter Olympic Games Organizing Committee (OCO '88), and The University of Calgary.